

# Vitreous bond silicon carbide wheel for grinding of silicon nitride

L.M. Xu<sup>a,1</sup>, Bin Shen<sup>b</sup>, Albert J. Shih<sup>b,\*</sup>

<sup>a</sup>Shanghai Jiao Tong University, Shanghai, China

<sup>b</sup>Department of Mechanical Engineering, University of Michigan, Ann Arbor, MI 48109 2136, USA

Received 25 April 2005; accepted 5 July 2005

Available online 19 August 2005

## Abstract

This study investigates the grinding of sintered silicon nitride using a SiC wheel with a fine abrasive grit size and dense vitreous bond. The difference of hardness between the green SiC abrasive and sintered Si<sub>3</sub>N<sub>4</sub> workpiece (25.5 vs. 13.7 GPa) is small. Large grinding forces, particularly the specific tangential grinding forces, are observed in SiC grinding of Si<sub>3</sub>N<sub>4</sub>. The measured specific grinding energy is high, 400–6000 J/mm<sup>3</sup>, and follows an inverse relationship relative to the maximum uncut chip thickness as observed in other grinding studies. The SiC wheel wears fast in grinding Si<sub>3</sub>N<sub>4</sub>. The *G*-ratio varies from 2 to 12. Two unique features in SiC grinding of Si<sub>3</sub>N<sub>4</sub> are the trend of increasing *G*-ratio at higher material removal rate and the excellent surface integrity, with 0.04–0.1 μm *R*<sub>a</sub> and no visible surface damage. For a specific material removal rate, surface cracks along the grinding direction are generated on the ground surface. The problem of chatter vibration was identified at high material removal rates. Periodic and uneven wheel loading marks and clusters of workpiece surface cracks across the grinding direction could be observed at high material removal rates. This study demonstrates that the SiC grinding wheel can be utilized for precision form grinding of Si<sub>3</sub>N<sub>4</sub> to achieve good surface integrity under a limited material removal rate.

© 2005 Elsevier Ltd. All rights reserved.

## 1. Introduction

Traditionally, diamond wheels are considered as the necessary tool for precision grinding of structural ceramics to the desired shape, dimension, and surface integrity. The discovery of silicon carbide (SiC) wheels with dense vitreous bond and fine grit size for grinding of zirconia has opened a new era for cost-effective, sub-μm precision production of ceramic components using the low-cost conventional abrasive [1–3]. Experimental results showed the *G*-ratio, which is defined as the volume of work-material removed vs. the volume of wheel wear, could be as high as 110 using a surface grinding machine (Harig) with relatively low stiffness (~6140 N/mm) [1] and over 500 using a cylindrical grinding machine (Studer S40) with good stiffness (~15,800 N/mm) [2]. The very low thermal conductivity of zirconia, about 2 W/m-K, and the relatively low thermal conductivity of SiC relative to diamond

(120 vs. 2300 W/m-K) cause a large fraction of heat to be retained in the chip. The large influx of heat in the chip softens the zirconia work-material for high efficiency grinding using SiC.

This hypothesis has been validated by measuring the flash temperature of SiC wheel grinding of zirconia [4]. The light emitted in the grinding zone transmits through the zirconia, which is semi-transparent in the infrared wavelength range, via an optical fiber, to a spectrometer. The measured flash temperature in SiC grinding of zirconia is high, about 3000 K, and independent of the downfeed and table speed in surface grinding. For diamond grinding of zirconia, the flash temperature is much lower. The melting temperature of the MgO partially stabilized zirconia is also about 3000 K [5]. This validates the hypothesis of high energy density in the zirconia chip generated by SiC grinding.

A unique feature of the SiC wheel is the high percentage of vitreous bond. During grinding, the dense vitreous bond is essential to provide adequate structural support on each abrasive grit to withstand the high grinding force and to prevent the grain pull-out.

In this study, the same vitreous bond SiC wheel is investigated for grinding of sintered silicon nitride (Si<sub>3</sub>N<sub>4</sub>)

\* Corresponding author. Tel.: +1 734 647 1766; fax: +1 734 936 0363.  
E-mail address: [shih@umich.edu](mailto:shih@umich.edu) (A.J. Shih).

<sup>1</sup> Research conducted as a visiting scholar at University of Michigan.

.  $\text{Si}_3\text{N}_4$  is a harder, more brittle, and more difficult to grind work-material than zirconia. The inherent difficulties arise from the very advantage that the  $\text{Si}_3\text{N}_4$  imparts to a wide range of industrial applications: high hardness resulting in superior wear resistance in extreme loading conditions.  $\text{Si}_3\text{N}_4$  has been widely used in the balls or rollers for the bearing and diesel engine plunger, pump, and cam follower applications [6]. It is also a good armor material [7]. The thermal conductivity of  $\text{Si}_3\text{N}_4$  is about 20–28 W/m-K, considerably higher than that of zirconia. The advantage of retaining heat in the chip to soften the work-material does not exist in SiC grinding of  $\text{Si}_3\text{N}_4$ . The  $G$ -ratio is expected to be low. However, the vitreous bond SiC wheel is low cost and can be precisely trued to complicated shape using either the stationary [8,9] or rotary [10] diamond tool for form grinding. The goal of this study is to explore the feasibility of using the dense vitreous bond SiC wheel for precision grinding of  $\text{Si}_3\text{N}_4$  components. The grinding forces, energy,  $G$ -ratio, and surface integrity are investigated.

In this paper, the surface grinding experiment set-up and procedure are first introduced. The grinding forces are measured. The specific grinding energy is calculated and compared to that of grinding zirconia. The wheel wear is measured and  $G$ -ratio is calculated. Finally, the surface roughness and integrity of ground  $\text{Si}_3\text{N}_4$  are examined and discussed.

## 2. Grinding experiment set-up and design

### 2.1. Grinding machine and set-up

The grinding experiments were conducted in an instrumented Chevalier Model Smart-B818 surface grinding machine with a 1.5 kW spindle. The set-up of the grinding experiment is shown in Fig. 1. The width and length of the workpiece surface for grinding are 6 and 20 mm, respectively. The vitreous bond grinding wheel, produced by Milacron, is comprised of green silicon

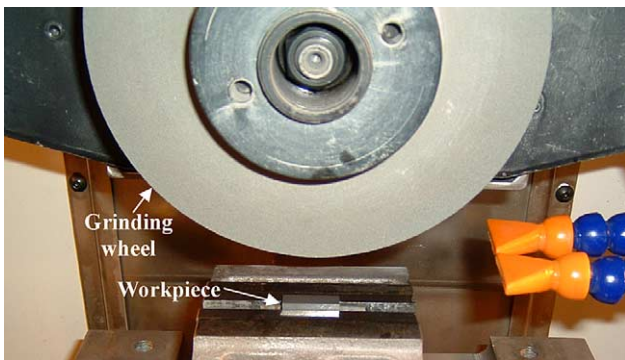


Fig. 1. Surface grinding experiment set-up and the silicon nitride workpiece (6 mm  $\times$  20 mm surface area).

carbide abrasive with 220 ANSI mesh size. The SiC wheel has a large percentage of vitreous bond (S grade hardness) and relatively low porosity. The size of grinding wheel is about 150 mm in diameter and 12.7 mm wide. The cutting fluid used in all grinding tests is the water-based Cimtech 500 synthetic cutting fluid at 5% concentration.

Truing the SiC wheel with dense vitreous bond using the stationary diamond tool has been studied [8,9]. The wear rate of diamond tool for truing this SiC wheel was relatively high, compared to truing other conventional abrasive wheels. In this study, a Norton (model CD8346 F022) single-point diamond was used for truing at 0.005 mm down feed and 100 mm/min traverse speed.

The normal and tangential grinding forces were measured using a Kistler Model 9257A piezoelectric dynamometer. The voltage signal from the dynamometer was amplified and acquired using a PC-based data acquisition system at 50 kHz sampling rate. Calibration tests were conducted to find the conversion factor from voltage to force. This grinding study uses a shallow down feed. The measured vertical and horizontal grinding forces are about the same as the normal and tangential grinding forces, respectively.

### 2.2. Workpiece, wheel wear measurement, and surface roughness

The workpiece is Toshiba TSN-10 sintered  $\text{Si}_3\text{N}_4$ . This material has 13.7 GPa Vickers hardness (500 g), 290 GPa Young's modulus, 6–7 MPa-m<sup>1/2</sup> fracture toughness, 3220 kg/m<sup>3</sup> density, 800 MPa bending strength, 680 J/kg-K specific heat, and 20 W/m-K thermal conductivity.

The wheel wear measurement method is the same as described in Refs. [1,15]. The wheel is 12.7 mm wide. The width of the part is narrower, 6 mm. A worn groove is generated on the wheel surface after grinding. A hard plastic part was ground to produce a replica of the worn grinding wheel. A Taylor Hobson Taylorsurf profilometer was used to measure the depth of wheel wear on the replica. Each  $G$ -ratio grinding test had to wear out about 6–22  $\mu\text{m}$  of the wheel to ensure the accuracy of  $G$ -ratio.

The same profilometer was used to measure the surface roughness of ground surfaces. Three measurement traces parallel and perpendicular to the grinding direction were measured. The average of the three arithmetic average surface roughness ( $R_a$ ) measurements along and across the grinding direction was used to represent the roughness of a ground surface.

### 2.3. Experimental procedures

Three grinding parameters investigated in this study are the down feed, table speed, and wheel surface speed. A baseline grinding test of four down feeds (2, 5, 10, and 15  $\mu\text{m}$ ), three table speeds (600, 2400, and 4200 mm/min),

and two wheel surface speeds (35 and 45 m/s) were conducted to investigate the grinding forces and surface integrity. In the baseline test, the grinding force and surface roughness were recorded.

Under the extreme grinding conditions of the down feed (2 and 15  $\mu\text{m}$ ), table speed (600 and 4200 m/min), and wheel surface speed (35 and 45 m/s), eight grinding tests were conducted to investigate the wheel wear ( $G$ -ratio) and surface integrity. The depth of wheel wear was measured. Ground surfaces were examined using the scanning electron microscopy (SEM) (Hitachi Model XL-30).

Three additional spark-out grinding tests were conducted at the lowest down feed (2  $\mu\text{m}$ ), 35 m/s wheel surface speed, and three table speeds (600, 2400, and 4200 m/min). Ten spark-out passes with zero down feed were performed at the end of each grinding cycle. The surface roughness and integrity were compared to that of ground surface without spark-out.

### 3. Grinding forces and specific grinding energy

Fig. 2 shows the specific grinding force vs. specific material removal rate (MRR) for the SiC wheel grinding of  $\text{Si}_3\text{N}_4$  at 35 and 45 m/s wheel surface speed. The zirconia grinding results, using the same SiC wheel at 39 m/s surface speed, were adopted from Ref. [1]. Specific grinding forces of 24 baseline tests, plotted at four different down feeds, are presented in Fig. 2.

Like in the zirconia grinding, high specific MRR generates high specific normal and tangential grinding forces. The specific normal grinding force is about 5–8 N/mm higher in grinding  $\text{Si}_3\text{N}_4$  than that in grinding zirconia. Very high specific tangential grinding force, more than twice of that in grinding zirconia, was observed. This reflects in the distinctively different levels of force ratio ( $F_N/F_T$ ): about five for zirconia grinding and lower than three for  $\text{Si}_3\text{N}_4$  grinding.

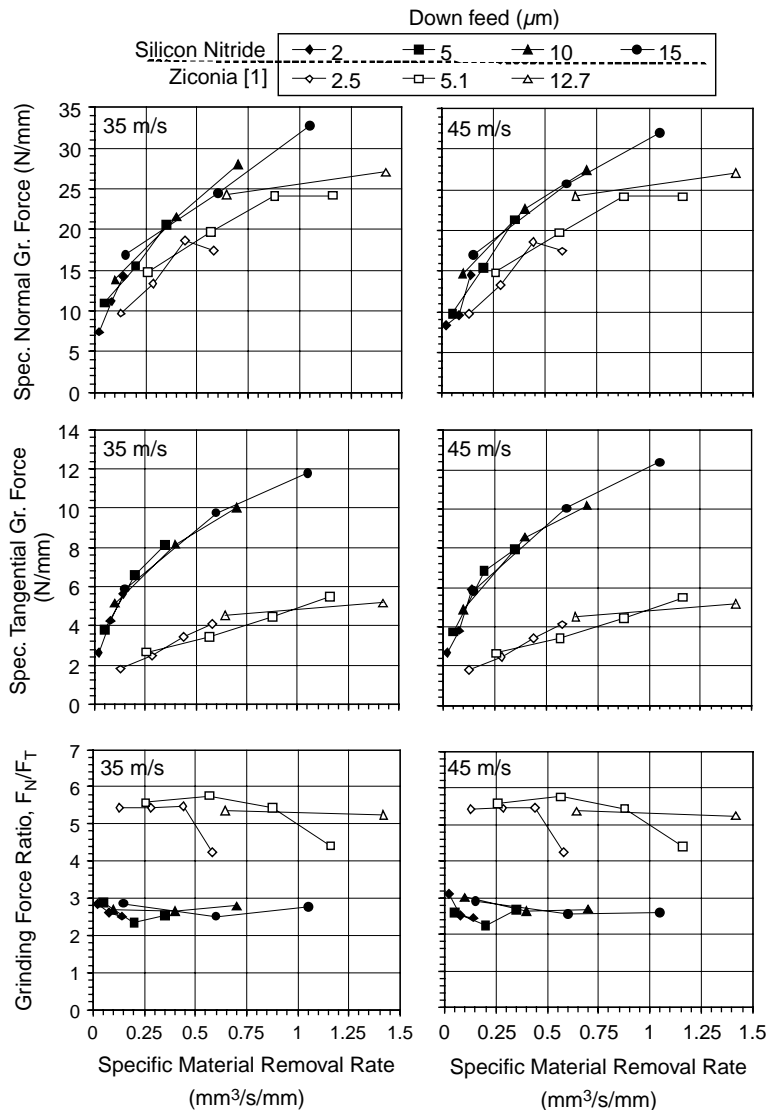


Fig. 2. Specific grinding forces and grinding force ratio for SiC grinding of silicon nitride and comparison with zirconia grinding results.

The vitreous bond CBN wheel for cylindrical grinding of the same  $\text{Si}_3\text{N}_4$  [11], which was conducted at  $7.6 \text{ mm}^3/\text{s}/\text{mm}$ , has about 14–24 N/mm specific normal grinding force, 2.5–4 N/mm specific tangential grinding force, and 4–5 force ratio. In comparison, the tangential grinding force is particularly high for SiC grinding of  $\text{Si}_3\text{N}_4$ . This is likely due to the lack of hardness of SiC abrasive grit producing a reduced capability to plow into  $\text{Si}_3\text{N}_4$  for effective work-material removal. The difference in hardness between green SiC (25.5 GPa) and  $\text{Si}_3\text{N}_4$  (13.7 GPa) is small. Such lack of abrasive hardness results in the high attrition wear of the SiC grit during grinding the  $\text{Si}_3\text{N}_4$  as well as the low  $G$ -ratio, which will be discussed later in Section 4.

The high tangential grinding force generates high grinding energy and a large amount of heat in the chip. The specific grinding energy,  $u$ , is determined from the tangential grinding force and wheel surface speed. The dimensionless specific grinding energy,  $u/H$ , i.e.  $u$  divided by the 13.7 GPa hardness of the sintered  $\text{Si}_3\text{N}_4$ , is plotted relative to the maximum uncut chip thickness,  $h_m$ , as shown in Fig. 3. The maximum uncut chip thickness,  $h_m$ , is defined in Ref. [12]:

$$h_m = \left[ \frac{3}{C \tan \theta} \left( \frac{v_w}{v_s} \right) \left( \frac{a}{d_s} \right)^{1/2} \right]^{1/2} \quad (1)$$

where  $C$  is the number of active cutting grains per  $\text{mm}^2$ ,  $\theta$  is the semi-included angle for the undeformed chip cross-section,  $v_w$  is the table speed,  $v_s$  is the wheel surface speed,

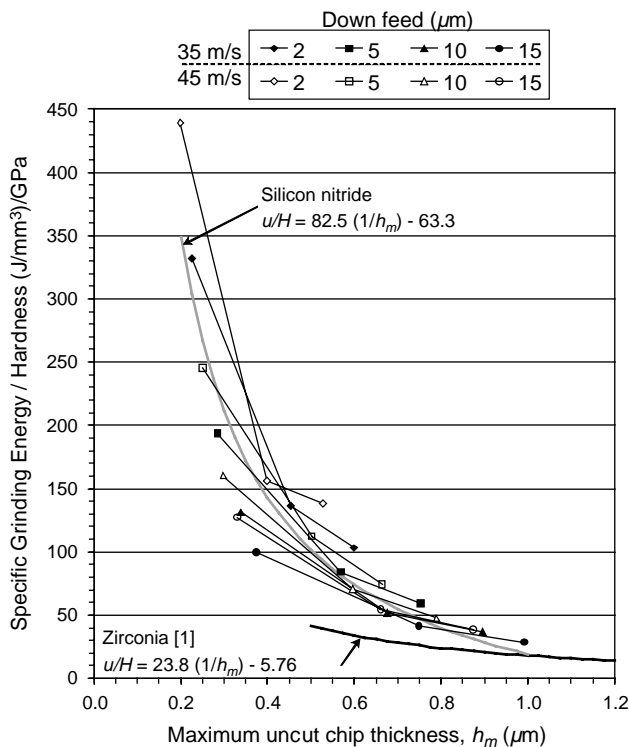


Fig. 3. Dimensionless specific grinding energy vs. maximum uncut chip thickness.

$a$  is the down feed, and  $d_s$  is the wheel diameter. In this study,  $C=35 \text{ mm}^{-2}$  is estimated from SEM micrographs of wheel surface, and  $\theta=60^\circ$  was used. The  $u/H$  vs.  $h_m$  for grinding of zirconia using the same SiC wheel [1] is also plotted for comparison.

As shown in Fig. 3,  $u/H$  ranges from 8.4 to 46 for SiC grinding of zirconia with 0.5–1.6  $\mu\text{m}$  maximum uncut chip thickness,  $h_m$ . This was already considered to be high compared to that for diamond grinding of  $\text{Si}_3\text{N}_4$  [13]. For SiC grinding of  $\text{Si}_3\text{N}_4$ , the  $u/H$  is even higher, ranging from 30 to 440 for  $h_m$  ranging from 0.25 to 1.0  $\mu\text{m}$ . An inverse relationship between  $u/H$  and  $h_m$ , similar to the same trend observed in other grinding studies [1,13,14], exists in this set of grinding test.

$$u/H = C_1/h_m + C_2 \quad (2)$$

where  $C_1$  and  $C_2$  are two parameters obtained from regression analysis. As shown in Fig. 3,  $C_1=82.5 \mu\text{m}$  and  $C_2=-63.3$ .

The  $u$  for SiC grinding of  $\text{Si}_3\text{N}_4$  ranging from 394 to  $6027 \text{ J/mm}^3$ , which is significantly higher than the 10 to  $800 \text{ J/mm}^3$  previously reported for diamond grinding of various types of  $\text{Si}_3\text{N}_4$  [14]. The highest specific grinding energy, over  $6000 \text{ J/mm}^3$ , for SiC grinding of  $\text{Si}_3\text{N}_4$  occurs at the lowest specific MRR. It is noted that the  $\text{Si}_3\text{N}_4$  dissociates at about  $1900^\circ\text{C}$  into Si and  $\text{N}_2$ . The specific energy required to sublimate the  $\text{Si}_3\text{N}_4$  from solid to gas phase is only about  $4 \text{ J/mm}^3$  [15]. SiC grinding certainly consumes a lot more energy than just the energy required to dissociate the  $\text{Si}_3\text{N}_4$  by heat.

#### 4. Wheel wear

Fig. 4 shows the  $G$ -ratio for grinding of  $\text{Si}_3\text{N}_4$  in six grinding tests. At the highest down feed (15  $\mu\text{m}$ ) and table speed (4200 mm/min), wheel loading and chatter vibration became severe problems. The wheel after grinding under such condition is shown in Fig. 5. A ring of uneven dark gray colored stripes, an obvious chatter vibration mark,

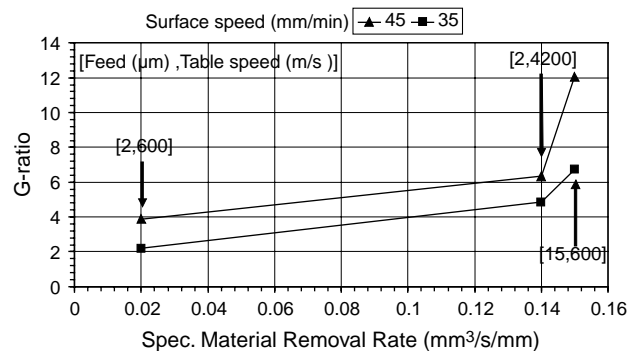


Fig. 4.  $G$ -ratio vs. specific material removal rate for SiC grinding of silicon nitride.





Fig. 5. The discoloration on the SiC wheel under high material removal rate (15  $\mu\text{m}$  down feed and 4200 mm/min table speed) showing the intermittent nature of the marks and indicating repeated contact and separation of workpiece and wheel.

was observed on the wheel surface. This discoloring is due to the  $\text{Si}_3\text{N}_4$  debris attached to the wheel surface. Grinding under such high MRR was not sustainable. The lack of effective hardness and ability of SiC to remove  $\text{Si}_3\text{N}_4$ , as discussed in Section 3, causes the high grinding force and chatter vibration between the wheel and workpiece and affects the surface roughness (Section 5) and integrity (Section 6).

The low  $G$ -ratio of 2 and 4 were observed at 35 and 45 m/s surface speed, respectively, in grinding at lowest specific MRR (0.02  $\text{mm}^3/\text{s}/\text{mm}$ ) under the 2  $\mu\text{m}$  down feed and 600 mm/min table speed. Such a low MRR, as presented in the following section, does not create surface cracks on the ground surface and has good surface roughness. It is a process parameter suitable for the finish grinding operation. At the higher specific MRRs, which generate higher grinding forces, the  $G$ -ratio is increased. This trend is the same as that observed in dense vitreous bond SiC grinding of zirconia, both in cylindrical and surface grinding configurations [1,2]. Such trend is opposite to what has been observed in traditional grinding wheel wear tests, in which the high MRR and high grinding force usually generate a low  $G$ -ratio. The brittle fracture of ceramic workpiece under the very high grinding force at high MRR promotes more effective material removal in SiC grinding of  $\text{Si}_3\text{N}_4$ . This is evident in the SEM observation of ground surfaces.

Attrition wear is expected to be the key wear mechanism of the SiC wheel. In each wheel wear grinding test, the groove depth of wear is about 6–19  $\mu\text{m}$ . This is smaller than the 76  $\mu\text{m}$  average size of the abrasive and indicates that significant abrasive grain pull-out does not happen in the dense vitreous bond SiC wheel.

## 5. Surface roughness

Fig. 6 shows the  $R_a$  of the ground surface along and across the grinding direction in 24 baseline tests and three spark-out grinding tests. Down feed affects the surface roughness significantly. Small down feed can achieve very

good surface roughness. At the smallest down feed (2  $\mu\text{m}$ ), the lower  $R_a$ , about 0.05  $\mu\text{m}$  along the grinding direction and 0.07–0.1  $\mu\text{m}$  across the grinding direction, can be achieved. The surface roughness along the grinding direction is consistently lower than that across the grinding direction in all grinding conditions. This is consistent with other surface grinding research [18]. Grinding direction has shown to affect the strength of ground  $\text{Si}_3\text{N}_4$  significantly [18,19].

For the same TSN-10  $\text{Si}_3\text{N}_4$ , 0.4–0.6  $\mu\text{m}$   $R_a$  was achieved in surface grinding using a metal bond, 320 ANSI mesh size diamond wheel [16] and 0.2–0.3  $\mu\text{m}$   $R_a$  was obtained in cylindrical grinding using a vitreous bond, 320 ANSI mesh size CBN wheel [17]. Note the grit size of diamond and CBN abrasive (320 ANSI mesh, 54  $\mu\text{m}$  average size) is smaller than that of the SiC abrasive (220 ANSI mesh, 76  $\mu\text{m}$  average size). Using the same SiC wheel for cylindrical grinding of zirconia, about 0.1–0.2  $\mu\text{m}$   $R_a$  can be achieved [2]. Overall, this study demonstrated that good surface roughness, about 0.05–0.1  $\mu\text{m}$   $R_a$  can be achieved in SiC grinding of  $\text{Si}_3\text{N}_4$  under low down feed and table speed.

The effect of table speed on surface roughness is mixed. At 35 m/s wheel surface speed, the surface roughness generally peaks with a 2400 mm/min table speed, i.e. the higher 4200 mm/min table speed helps reduce the surface roughness. At 45 m/s wheel surface speed, however, high table speed generally deteriorates the surface roughness. Better surface roughness can be achieved at low, 600 mm/min, table speed.

The effect of wheel surface speed on surface roughness is significant at high table speed. This is due to the severe damage of the ground surface at high MRR, as will be revealed by SEM analysis of ground surfaces in the following section.

The cross symbols in Fig. 6 show that the spark-out further reduces the surface roughness along the grinding direction to 0.04  $\mu\text{m}$   $R_a$ , independent of the table speed. Across the grinding direction, the spark-out does not significantly change the  $R_a$ , which is constant at the 0.11  $\mu\text{m}$  level. Such fine surface roughness is close to

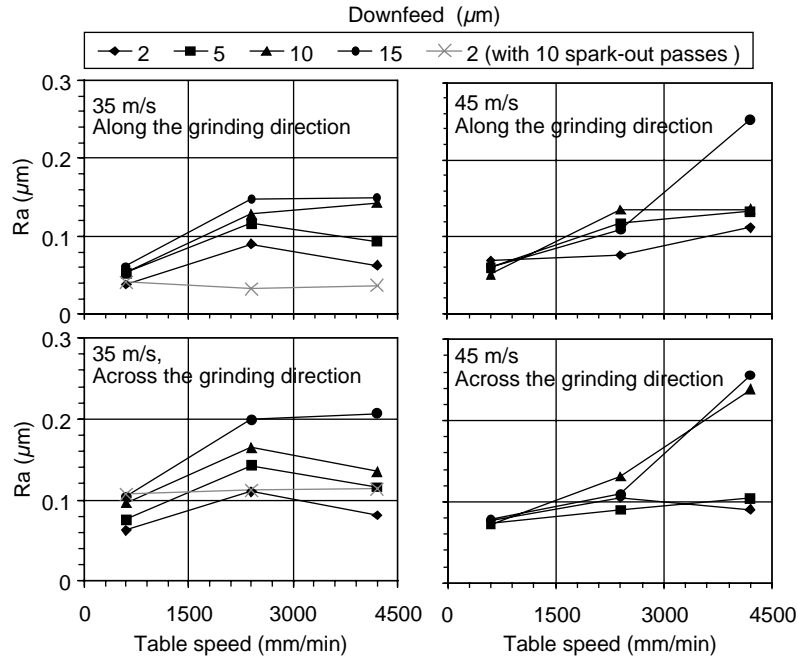


Fig. 6. Surface roughness for SiC grinding of silicon nitride.

the resin bond diamond wheel with fine abrasive size for high speed grinding of  $\text{Si}_3\text{N}_4$  [20].

## 6. SEM analysis and grinding damages

The grinding surface and subsurface damage of  $\text{Si}_3\text{N}_4$  have been well studied. The material removal mechanism [21], crack depth and formation [22], and pulverization and void formation [23–25] on ground  $\text{Si}_3\text{N}_4$  surfaces have been investigated.

Fig. 7 presents SEM micrographs of ground surfaces under the highest and lowest down feed (2 and 15  $\mu\text{m}$ ), table speed (600 and 4200 mm/min), and wheel surface speed (35 and 45 m/s). The level of magnification ( $600\times$ ) is the same for all SEM micrographs for mutual comparison. The specific MRR,  $h_m$ , and  $R_a$  along and across the grinding direction are also listed next to each SEM micrograph.

For grinding at the lowest down feed (2  $\mu\text{m}$ ), table speed (600 mm/min), and wheel surface speed (35 m/s), no visible surface crack can be observed. At high magnification ( $1200\times$ ), no visible surface cracks or pulverized surface layer can be recognized. The surface roughness is low, 0.038 and 0.063  $\mu\text{m}$   $R_a$  along and across the grinding direction, respectively. This is close to the ductile-regime grinding [26].

The increase in wheel surface speed reduces the  $h_m$ , but increases the wheel vibration, particularly for the grinding machine used in this study without active wheel balancing. Under the lowest down feed and table speed, the increase of wheel surface speed to 45 m/s reduces the  $h_m$  (to 0.2  $\mu\text{m}$ )

but the surface roughness slightly deteriorates, likely due to an increase in wheel vibration.

The increase of table speed from 600 to 4200 mm/min for 2  $\mu\text{m}$  down feed and 35 m/s wheel surface speed increases the  $h_m$  to 0.60  $\mu\text{m}$  and generates visible surface cracks along the grinding direction. This is the median crack caused by the scribing of SiC abrasive on  $\text{Si}_3\text{N}_4$  surface during grinding. Besides cracks, the surface roughness is increased in both directions and pulverization damage can be observed on the ground surface.

Under the same table speed (4200 mm/min) and down feed (2  $\mu\text{m}$ ), the increase of wheel surface speed to 45 m/s further deteriorates the surface integrity. The increase of down feed to 15  $\mu\text{m}$  also increases the  $h_m$  and generates cracks along the grinding direction. Surface cracks may help to improve the  $G$ -ratio in grinding at high MRR (Fig. 4).

At the highest down feed (15  $\mu\text{m}$ ) and table speed (4200 mm/min), the orientation of cracks changes to across the grinding direction. Under such high material removal rate grinding, a cluster of cracks across the grinding direction is observed. Fig. 8 shows a lower magnification ( $50\times$ ) SEM micrograph of the surface ground at the highest MRR and 35 m/s wheel surface speed. The corresponding grinding wheel surface after such grinding condition is shown in Fig. 5. Chatter vibration of the wheel is expected to cause significant variation in the uncut chip thickness and the impact of abrasive grains engaged in material removal. The SiC on the wheel surface is expected to have a large wear flat area. The impact of SiC abrasive grain on the ground  $\text{Si}_3\text{N}_4$  surface is the likely source of surface cracks across the grinding direction.

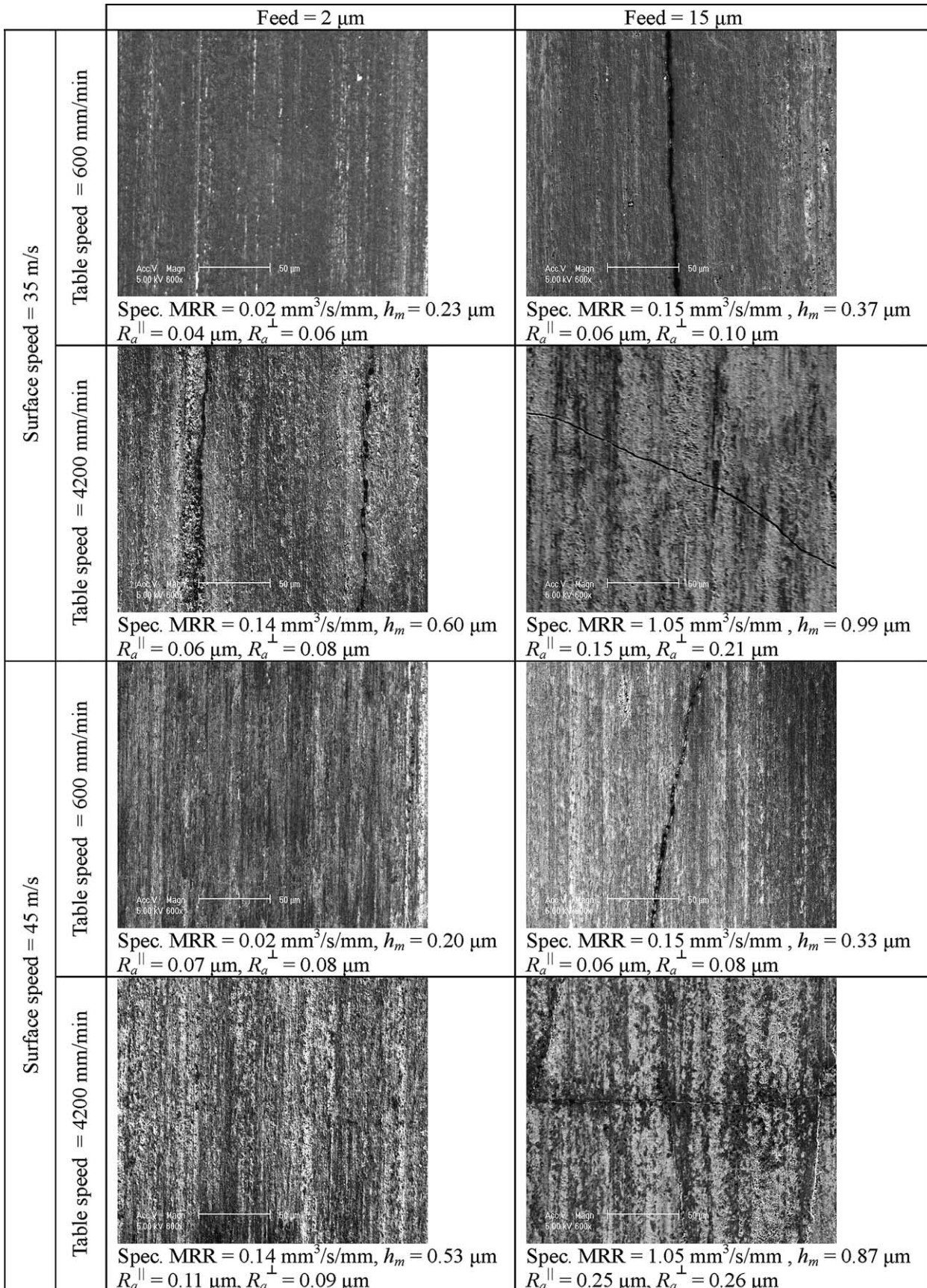


Fig. 7. SEM micrographs of ground silicon nitride surface. Note:  $R_a^{\parallel}$  is measured along and  $R_a^{\perp}$  is measured across the grinding direction.



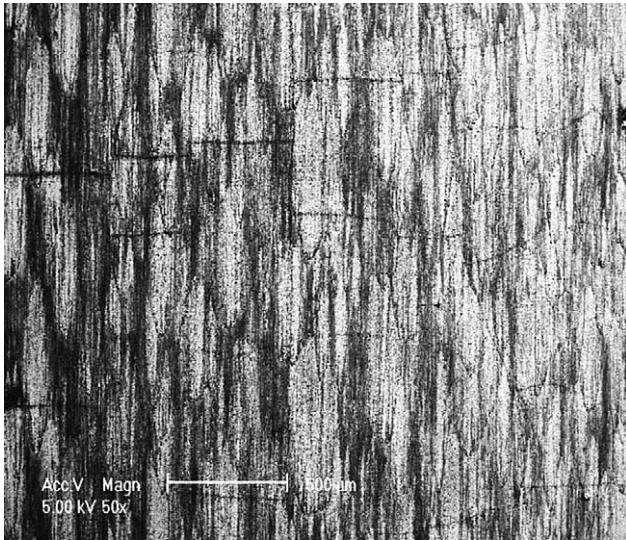


Fig. 8. The silicon nitride surface ground at the highest material removal rate (15  $\mu\text{m}$  down feed and 4200 mm/min table speed) and 35 m/s wheel surface speed (surface roughness:  $R_a = 0.15 \mu\text{m}$  along grinding direction and 0.21  $\mu\text{m}$  across grinding direction).

SEM micrographs of the three ground surface with 10 spark-out passes show no visible crack or pulverized surface layer under the high magnification (1200 $\times$ ). These three parts, as indicated by cross-symbols in Fig. 6, have mirror-like surface with low surface roughness in the range of 0.03–0.04  $\mu\text{m}$   $R_a$  along and 0.11  $\mu\text{m}$   $R_a$  across the grinding direction. A unique advantage of the SiC is the lack of hardness to severely damage the  $\text{Si}_3\text{N}_4$ . Although such lack of abrasive hardness was not good from the wheel wear perspective, it is beneficial to generate a damage-free surface with low  $R_a$ . Mirror-like surfaces with complicated shapes have been demonstrated in SiC grinding of  $\text{Si}_3\text{N}_4$  in applications for diesel engine fuel systems.

## 7. Concluding remarks

The SiC wheel with small, 220 ANSI mesh, size abrasive and dense vitreous bond was studied for grinding of sintered  $\text{Si}_3\text{N}_4$ . Very good surface roughness (0.04  $\mu\text{m}$   $R_a$  along the grinding direction and 0.1  $\mu\text{m}$   $R_a$  across the grinding direction) without apparent cracks on the surface could be observed on the surface ground by SiC wheel with low MRR. The  $G$ -ratio under such grinding condition was low, about 2 and 4 under 35 and 45 m/s wheel surface speed, respectively. At slightly higher specific MRR (0.14  $\text{mm}^3/\text{s}/\text{mm}$ ), the surface started to exhibit cracks along the grinding direction and the  $G$ -ratio was increased to about 12–14. When the specific MRR was increased to 1.05  $\text{mm}^3/\text{s}/\text{mm}$ , severe chatter vibration occurred, uneven and severe wheel loading on the wheel surface could be observed, and clusters of cracks across the grinding

direction were examined on ground surfaces. The grinding under such high MRR was not sustainable.

The vitreous bond SiC wheel is inexpensive, more than an order of magnitude lower in cost than the diamond or CBN wheels. Two other benefits of the SiC wheel have been proven beneficial in implementation of this process for production grinding of structural ceramics. One is the ability to use existing grinding machines with the stationary diamond truing and dressing tool. No additional capital investment is required to modify the machine by adding the rotary truing device for superabrasive grinding. The other benefit is the ability to true the SiC wheel to precise and complicate shape for form grinding. It is difficult to precisely shape the diamond wheel using a diamond tool [27] and the cost of CBN wheel is high. Both prohibit the precise form grinding of ceramics. SiC wheel grinding provides an alternative way for cost-effective precision form grinding of  $\text{Si}_3\text{N}_4$  and zirconia structural ceramics.

The grinding forces in SiC grinding of  $\text{Si}_3\text{N}_4$  are very high. To achieve the best results in both  $G$ -ratio (wheel wear) and surface integrity, the stiffness of the grinding machine is critical. It is believed that higher  $G$ -ratio than the values observed in this study can be achieved using a stiffer, more precise grinding machine. The vibration observed in grinding using the dense vitreous bond SiC wheel is also identified as an important area of improvement, particularly for grinding at the high material removal rate.

## Acknowledgements

This research is sponsored by the National Science Foundation DMII Grant #9983572 and #0422947 and Powerix Technology. Assistance from Jie Feng is greatly appreciated.

## References

- [1] A.J. Shih, A.C. Curry, R.O. Scattergood, T.M. Yonushonis, D.J. Gust, M.B. Grant, S.B. McSpadden, T. Watkins, Cost-effective grinding of zirconia using the dense vitreous bond silicon carbide wheel, *Journal of Manufacturing Science and Engineering* 125 (2003) 297–303.
- [2] A.J. Shih, T.M. Yonushonis, High infeed rate method for grinding ceramic workpiece with silicon carbide grinding wheels, US Patent Number 6,030,277 (2000).
- [3] A.J. Shih, T.M. Yonushonis, High infeed rate method for grinding ceramic workpiece with silicon carbide grinding wheels, US Patent Number 6,220,933 (2001).
- [4] A.C. Curry, A.J. Shih, R.O. Scattergood, J. Kong, S.B. McSpadden, Grinding temperature measurements in MgO PSZ using infrared spectrometry, *Journal of the American Ceramic Society* 86 (2003) 333–341.
- [5] R. Stevens, Zirconia and Zirconia Ceramics Magnesium Elektron Publication No. 113, Magnesium Elektron Ltd, Manchester, UK, 1986.



- [6] W.F. Mandler, T.M. Yonushonis, K. Shinosawa, Ceramic successes in diesel engines, 6th International Symposia on Ceramic Materials and Components for Engines, Arita-Machi, Japan, 19–23 (1997).
- [7] J.W. McCauley, A.M. Rajendran, W. Gooch, S. Bless, K.V. Logan, M. Normandia, S. Wax, Ceramic Armor Materials by Design, Ceramic Transactions, vol. 134.
- [8] A.J. Shih, L. Akemon, Wear of the blade diamond tools in truing vitreous bond grinding wheels, part I - wear measurement and results, *Wear* 250 (2001) 587–592.
- [9] A.J. Shih, W.I. Clark, L. Akemon, Wear of the blade diamond tools in truing vitreous bond grinding wheels, part II—truing and grinding forces and wear mechanism, *Wear* 250 (2001) 593–603.
- [10] A.J. Shih, An experimental investigation of rotary truing and dressing of vitreous bond wheels for ceramic grinding, *International Journal of Machine Tools and Manufacture* 40 (2000) 1755–1774.
- [11] A.J. Shih, M.B. Grant, T.M. Yonushonis, T.O. Morris, S.B. McSpadden, High speed and high material removal rate grinding of ceramics using the vitreous bond CBN wheel, *Machining Science and Technology* 4 (2000) 43–58.
- [12] S. Malkin, Grinding technology, Theory and Application of Machining with Abrasives, Ellis Horwood, p. 26.
- [13] T.W. Hwang, C.J. Evans, S. Malkin, Size effect for specific energy in grinding of silicon nitride, *Wear* 225–229 (1999) 862–867.
- [14] T.W. Hwang, S. Malkin, Grinding mechanisms for ceramics, *CIRP Annals* 45 (1996) 569–580.
- [15] G.S. Brady, H.R. Clauser, *Materials Handbook*, Twelfth ed., McGraw-Hill.
- [16] B.K. Rhoney, A.J. Shih, R.O. Scattergood, J.L. Akemon, D.J. Gust, B. Grant, Wire electrical discharge machining of metal bond diamond wheels for ceramic grinding, *International Journal of Machine Tool and Manufacture* 42 (2002) 1355–1362.
- [17] A.J. Shih, M.B. Grant, T.M. Yonushonis, T.O. Morris, S.B. McSpadden, High speed and high material removal rate grinding of ceramics using the vitreous bond CBN wheel, *Machining Science and Technology* 4 (1) (2000) 43–58.
- [18] T.J. Strakna, S. Jahanmir, R.L. Allor, K. Kumar, Influence of grinding direction on fracture strength of silicon nitride, *Journal of Engineering Materials and Technology* 118 (3) (1996) 335–342.
- [19] W. Pfeiffer, T. Hollstein, Influence of grinding parameters on strength-dominating near-surface characteristics of silicon nitride ceramics, *Journal of the European Ceramic Society* 17 (1997) 487–494.
- [20] H. Huang, L. Yin, L. Zhou, High speed grinding of silicon nitride with resin bond diamond wheels, *Journal of Materials Processing Technology* 141 (2003) 329–336.
- [21] H.H.K. Xu, S. Jahanmir, L.K. Ives, Material removal and damage formation mechanisms in grinding silicon nitride, *Journal of Materials Research* 11 (7) (1996) 1717–1724.
- [22] T.M.A. Maksoud, A.A. Mokbel, J.E. Morgan, Evaluation of surface and sub-surface cracks of ground ceramics, *Journal of Materials Processing Technology* 88 (1999) 222–243.
- [23] B. Zhang, T.D. Howes, Material removal mechanisms in grinding ceramics, *Annals of the CIRP* 43 (1994) 305–308.
- [24] B. Zhang, T.D. Howes, Subsurface evaluation of ground ceramics, *Annals of the CIRP* 44 (1995) 263–266.
- [25] B. Zhang, X.L. Zheng, H. Tokura, M. Yoshikawa, Grinding induced damage in ceramics, *Journal of Materials Processing Technology* 132 (2003) 353–364.
- [26] T.G. Bifano, T.A. Dow, R.O. Scattergood, Ductile-regime grinding: a new technology for machining brittle materials, *Journal of Engineering for Industry* 113 (1991) 184–189.
- [27] A.J. Shih, Rotary truing of the vitreous bond diamond grinding wheels using metal bond diamond disks, *Machining Science and Technology* 2 (1998) 13–28.